Statistics and Its Interface Volume 12 (2019) 295–307

Objective Bayesian analysis for accelerated degradation data using inverse Gaussian process models*

Lei He, Dongchu Sun, and Daojiang He†

The inverse Gaussian (IG) process has become an important family in degradation analysis. In this paper, we propose an objective Bayesian method to analyze the constant-stress accelerated degradation test (CSADT) based on IG process model. Several commonly used noninformative priors, including the Jeffreys prior, the reference prior and the probability matching prior, are derived after reparameterization. The propriety of the posteriors under those priors is validated, among which two types of reference priors are shown to yield improper posteriors while the others can lead to proper posteriors. A simulation study is carried out to compare the proposed Bayesian method with the maximum likelihood one in terms of the mean squared errors and the frequentist coverage probability. Finally, the approach is applied to a real data example and the mean-time-to-failure of the product under the usage stress is estimated.

AMS 2000 subject classifications: Primary 62F15; secondary 62N05.
Keywords and phrases: Accelerated degradation test, Inverse Gaussian process, Mean-time-to-failure, Objective Bayes.

1. INTRODUCTION

To address the fierce competition in markets and meet the demands of customers, manufacturers are often required to evaluate the reliability of their products rapidly and efficiently. For highly reliable products, however, it is quite difficult to obtain sufficient time-to-failure data through traditional life tests during a short of time period. Moreover, even applying accelerated life tests, which are designed to test products at harsher conditions (such as higher temperature or voltage), the performance of failure is still not good enough within a reasonable testing duration. In such restraints, if there is a quality characteristic, whose degradation over time could reveal the failure behavior of a product, then an alternative approach is to collect sufficient degradation data at higher levels of stress to predict the product's lifetime information under the usage stress. Such tests are called accelerated degradation tests (ADTs), general references are included in [15] and [16].

It is well known that ADTs are able to greatly save time and expenses than traditional degradation tests, so ADTs have attracted much attention in practice. For accelerated degradation analysis, a crucial issue is how to establish an appropriate model to characterise the product's degradation path. The typical and popular model for analyzing ADTs is stochastic process model, which is to utilize a time-dependent structure to describe the changes in degradation over time. The Wiener process is a frequently used stochastic process model in practical applications. For instance, Whitmore [26] proposed a basic Wiener process for degradation modeling of the declining gain of a transistor, and subsequently, Whitmore and Schenkelberg [27] applied the same model to analyze the resistance increase in a self-regulating heating cable. For some recent developments on the Wiener degradation model, one can see [11], [24], [31] and references therein. As Tsai, Tseng and Balakrishnan [20] pointed out, however, the Gamma process is more suitable for describing the product's degradation path compared with the Wiener process when the degradation path is a strictly increasing pattern. Bagdonavičius and Nikulin [2] constructed a degradation model based on the Gamma process with time-dependent explanatory variables to illustrate traumatic events. Lawless and Crowder [13] proposed a tractable Gamma process with random effects to analyze crack growth data. Extensional research on the Gamma process can be found in [14], [18] and [21] among others.

Recently, Wang and Xu [23] found that the Weiner process and the Gamma process cannot fit well the GaAs laser degradation data in [15]. A more efficient method for degradation modeling is to use the inverse Gaussian (IG) process originally proposed by Wasan [25]. Ye and Chen [29] systematically investigated the IG process, and showed that the IG process has many superb properties when dealing with random effects and covariates. Some other ADT models based

*Dongchu Sun's work is supported by the National Science Foundation of United States (Grant No. SES-1260806), the Chinese 111 Project (Grant N0. B14019) and the National Natural Science Foundation of China (Grant No. 11671146); Daojiang He's work is supported by the National Natural Science Foundation of China (Grant No. 11201005) and the Humanities and Social Sciences Foundation of Ministry of Education, China (Grant No. 17YJC910003).
†Corresponding author.

on the assumption of IG process have also been developed, one may refer to [22] and [30].

Note that the approaches considered in the aforementioned references are mainly from frequentist points of view or subjective Bayesian methods. However, the objective Bayesian approach has also many advantages in the statistical analysis. One of the most appealing feature is the use of noninformative priors, which include the Jeffreys prior, the reference priors and the probability matching priors, see [3] for more details. Following this topic, Xu and Tang [28] proposed an objective Bayesian analysis for a linear degradation model. This approach is further adopted in [9] and [10]. In this paper, we will present an objective Bayesian method to analyze the constant-stress acceleration degradation test (CSADT) using an IG process model. Our aim is to provide noninformative priors for the model that do result in proper posteriors and that enable Bayesian inferences.

The remainder of this paper is organized as follows. In Section 2, the IG process model is introduced and the mean-time-to-failure (MTTF) of the product under various stresses are given. In Section 3, several noninformative priors are derived after reparameterization. In Section 4, the propriety of the posterior distributions under these priors is validated, and a Monte Carlo procedure is proposed to generate the samples from the proper posteriors. In Section 5, a simulation study is carried out to show the performance of the derived priors. A real data set from [15] is analyzed in Section 6 via the proposed method. Finally, some concluding remarks are given in Section 7; proofs of the main theorems are presented in Appendix A.

2. THE IG PROCESS MODEL

Consider the degradation characteristic $Y(t)$ of a product which is measurable at time t, and assume that $Y(t)$ follows an IG process with $Y(0) = 0$, i.e.,

$$Y(t) \sim \mathcal{IG}(\eta t, \sigma t^2), \tag{1}$$

where η and σ are two unknown parameters to be estimated, and $\mathcal{IG}(a, b)$, $a, b > 0$, denotes the IG distribution with probability density function (PDF)

$$f_{\mathcal{IG}}(y; a, b) = \sqrt{\frac{b}{2\pi y^3}} \exp\left\{-\frac{b(y-a)^2}{2a^2 y}\right\}.$$

Then, it is readily seen that $Y(t)$ satisfies the following properties: (i) $Y(t)$ has statistically independent increments, that is, $Y(t_2)-Y(t_1)$ and $Y(t_4)-Y(t_3)$ are mutually independent for $\forall t_4 > t_3 \geq t_2 > t_1 > 0$. (ii) For $\forall t > s$, the increment $Y(t) - Y(s)$ follows an IG distribution $\mathcal{IG}(\eta\lambda, \sigma\lambda^2)$, where $\lambda = t - s$.

Assume that there are n_i units available for the CSADT that use the stress level S_i, $i = 1, 2, \cdots, r$. For fixed i, let m_{ij} be the number of measurements for the jth unit at the stress level S_i, $j = 1, 2, \cdots, n_i$. Given i and j, denote y_{ijk} by the degradation characteristic measured at time t_{ijk} for $k = 1, 2, \cdots, m_{ij}$, where $t_{ij1} < t_{ij2} < \cdots < t_{ijm_{ij}}$ are the ordered observation times. Then each degradation increment $\Delta y_{ijk} = y_{ijk} - y_{ij,k-1}$ follows an IG distribution $\mathcal{IG}(\eta_i \lambda_{ijk}, \sigma\lambda_{ijk}^2)$, where $\lambda_{ijk} = t_{ijk} - t_{ij,k-1}$ and $t_{ij0} = 0$.

Under the stress S_i, the time-to-failure is defined as the moment that the corresponding degradation process $Y_i(t)$ first reaches a critical value $\nu > 0$, say τ_i, then

$$\tau_i = \inf\{t \geq 0 | Y_i(t) \geq \nu\}.$$

Following Peng [19], the MTTF under the stress S_i, $i = 0, 1, \cdots, r$, can be represented as

$$\text{MTTF}_i = \left(\frac{\nu}{\eta_i} + \frac{\eta_i}{\sigma}\right) \Phi\left(\frac{\sqrt{\sigma\nu}}{\eta_i}\right) + \sqrt{\frac{\nu}{\sigma}}\phi\left(\frac{\sqrt{\sigma\nu}}{\eta_i}\right) - \frac{\eta_i}{2\sigma}, \tag{2}$$

where S_0 stands for the usage stress level, and $\Phi(x)$ and $\phi(x)$ are the cumulative distribution function and the PDF of the standard normal distribution, respectively. In this paper, we assume that the accelerating function is log-linear, i.e.,

$$\log(\eta_i) = v_0 + v_1 \varphi(S_i), \quad i = 0, 1, \cdots, r, \tag{3}$$

where v_0 and $v_1 > 0$ are unknown parameters to be estimated, and $\varphi(S_i)$ is a given function of stress level S_i. In particular, $\varphi(x) = -\log(x)$ for typical inverse power law relation, $\varphi(x) = 1/x$ for Arrhenius relation and $\varphi(x) = x$ for exponential relation, see [30]. Under this assumption, the parameter σ does not depend on stress S_i, but the degradation speed and the degradation volatility increase with the stress S_i, since the mean and the variance of Δy_{ijk} are $\eta_i \lambda_{ijk}$ and $\eta_i^3 \lambda_{ijk}/\sigma$, respectively.

In CSADTs, we are interested in the MTTF of the product under the usage stress S_0. In other words, the parameters η_0 and σ in (2) are of interest for statistical inferences. Similar to [9], we consider the following reparameterization scheme for the parameters η_i's. Let

$$\eta_i = \eta_0 \theta^{h_i}, \quad i = 1, \cdots, r, \tag{4}$$

where $\theta = \exp\{v_1[\varphi(S_1) - \varphi(S_0)]\} = \frac{\eta_1}{\eta_0} > 1$ is the acceleration factor from stress S_0 to S_1, and

$$h_i = \frac{\varphi(S_i) - \varphi(S_0)}{\varphi(S_1) - \varphi(S_0)}.$$

Obviously, we have $h_r > h_{r-1} > \cdots > h_1 = 1$. Now, the new parameters to be estimated are $\vartheta = (\eta_0, \theta, \sigma)$, and the likelihood function of ϑ based on $\boldsymbol{y} = \{\Delta y_{ijk},\ i = 1, 2, \cdots, r;\ j = 1, 2, \cdots, n_i;\ k = 1, 2, \cdots, m_{ij}\}$ is given by

$$L(\vartheta|\boldsymbol{y}) = \prod_{i=1}^{r}\prod_{j=1}^{n_i}\prod_{k=1}^{m_{ij}} \sqrt{\frac{\sigma\lambda_{ijk}^2}{2\pi y_{ijk}^3}} \exp\left\{-\frac{\sigma(y_{ijk} - \eta_0\theta^{h_i}\lambda_{ijk})^2}{2\eta_0^2\theta^{2h_i} y_{ijk}}\right\}. \tag{5}$$

3. NONINFORMATIVE PRIORS

In this section, we will derive several important noninformative priors for the parameters (η_0, θ, σ) in the IG process model, including the Jeffreys prior, the reference priors and the probability matching priors.

3.1 The Jeffreys prior

The Jeffreys prior, as we know, is proportional to the squared root of the determinant of the Fisher information matrix (see [12]). So the primary work is to derive the Fisher information matrix of the parameters.

Theorem 3.1. *The Fisher information matrix of* $\vartheta = (\eta_0, \theta, \sigma)$ *is of the following form:*

$$H(\vartheta) = \begin{pmatrix} \sum_{i=1}^{r} \frac{\sigma\lambda_i}{\eta_0^3\theta^{h_i}} & \sum_{i=1}^{r} \frac{\sigma h_i\lambda_i}{\eta_0^2\theta^{h_i+1}} & 0 \\ \sum_{i=1}^{r} \frac{\sigma h_i\lambda_i}{\eta_0^2\theta^{h_i+1}} & \sum_{i=1}^{r} \frac{\sigma h_i^2\lambda_i}{\eta_0\theta^{h_i+2}} & 0 \\ 0 & 0 & \frac{N}{2\sigma^2} \end{pmatrix},$$

where $N = \sum_{i=1}^{r}\sum_{j=1}^{n_i} m_{ij}$ *and* $\lambda_i = \sum_{j=1}^{n_i}\sum_{k=1}^{m_{ij}} \lambda_{ijk}$.

According to Theorem 3.1, the Jeffreys prior for (η_0, θ, σ) is

$$\pi_J(\eta_0, \theta, \sigma) \propto \eta_0^{-2}\sqrt{a(\theta)}, \tag{6}$$

where

$$a(\theta) = \sum_{1\le i<j\le r} \frac{\lambda_i\lambda_j(h_i - h_j)^2}{\theta^{h_i+h_j+2}}. \tag{7}$$

3.2 The reference priors

The reference prior proposed by Bernardo [5] is an alternative method for deriving noninformative priors, the key feature of which is to separate the parameters into several different group ordering of interest. In fact, the group ordering of the parameters reflects the inferential importance of parameters. For more details, see [4].

In our problem, η_0 and σ are two parameters of interest. Therefore, we first consider three possible group orderings for the parameters (η_0, θ, σ), namely $\{\eta_0, \sigma, \theta\}$, $\{\sigma, \eta_0, \theta\}$ and $\{(\eta_0, \sigma), \theta\}$. It turns out that two types of reference priors can be yielded, which are summarized in the following theorem.

Theorem 3.2. *Suppose that the sampling distribution is given by* (5)*, then the reference priors with the group orderings* $\{\eta_0, \sigma, \theta\}$ *and* $\{\sigma, \eta_0, \theta\}$ *are the same and given by*

$$\pi_{R_1}(\eta_0, \theta, \sigma) \propto \eta_0^{-\frac{3}{2}}\sigma^{-1}\sqrt{b(\theta)},$$

whereas the reference prior with the group ordering $\{(\eta_0, \sigma), \theta\}$ *has the following form*

$$\pi_{R_2}(\eta_0, \theta, \sigma) \propto \eta_0^{-\frac{3}{2}}\sigma^{-\frac{1}{2}}\sqrt{b(\theta)},$$

where

$$b(\theta) = \sum_{i=1}^{r} \frac{h_i^2\lambda_i}{\theta^{h_i+2}}. \tag{8}$$

Remark 1. The reference priors for the group orderings $\{(\eta_0, \theta), \sigma\}$ and $\{\sigma, (\eta_0, \theta)\}$ are the same as the Jeffreys prior π_J, since the Fisher information matrix of (η_0, θ, σ) satisfies the conditions of Theorem 1 in [6]. In addition, the reference prior is π_{R_1} when the group ordering is $\{\eta_0, \theta, \sigma\}$.

Remark 2. For comparison, another type of reference prior will be considered here. For the group orderings $\{\theta, \eta_0, \sigma\}$, $\{\theta, \sigma, \eta_0\}$ and $\{\sigma, \theta, \eta_0\}$, the reference priors are the same and of the form

$$\pi_{R_3}(\eta_0, \theta, \sigma) \propto \eta_0^{-\frac{3}{2}}\sigma^{-1}\sqrt{\frac{a(\theta)}{c(\theta)}},$$

where $a(\theta)$ is defined in (7), and

$$c(\theta) = \sum_{i=1}^{r} \frac{\lambda_i}{\theta^{h_i}}.$$

3.3 The probability matching priors

In this subsection, we are mainly devoted to derive the probability matching priors for multiple parametric functions of interest. It is well known that the probability matching priors are such that the joint posterior distribution function matches, up to $O(n^{-1})$, with the corresponding frequentist distribution function (see [7]). In our problem, both of parametric functions $\phi_1(\vartheta) = \eta_0$ and $\phi_2(\vartheta) = \sigma$ are of interest. Therefore, we can obtain a simultaneous marginal probability matching prior $\pi_M(\vartheta)$ for parametric functions $\phi_1(\vartheta)$ and $\phi_2(\vartheta)$, which must satisfy the following partial differential equations

$$\sum_{\kappa=1}^{3} D_\kappa\{\epsilon_{j\kappa}(\vartheta)\pi_M(\vartheta)\} = 0, \quad j = 1, 2, \tag{9}$$

where $D_\kappa = \partial/\partial\vartheta_\kappa$ with $\vartheta_1 = \eta_0, \vartheta_2 = \sigma$ and $\vartheta_3 = \theta$, and

$$\epsilon_j(\vartheta) = (\epsilon_{j1}(\vartheta), \epsilon_{j2}(\vartheta), \epsilon_{j3}(\vartheta))^T = \frac{H^{-1}(\vartheta)\nabla_{\phi_j}(\vartheta)}{\sqrt{\nabla_{\phi_j}^T(\vartheta)H^{-1}(\vartheta)\nabla_{\phi_j}(\vartheta)}},$$

here the symbol $\nabla_{\phi_j}(\vartheta)$ represents the gradient vector of $\phi_j(\vartheta)$ with $j = 1, 2$, and the inverse of the Fisher information matrix $H^{-1}(\vartheta)$ is defined in (14).

For this we have the following theorem, the proof of which can be established by solving the equations (9).

Theorem 3.3. *When η_0 and σ are of interest and θ is a nuisance parameter, the probability matching prior is*

$$\pi_M(\vartheta) = \sigma^{-1} g\left(\eta_0 \exp\left\{\int \frac{b(\theta)}{d(\theta)} d\theta\right\}\right) \cdot \exp\left\{\frac{3}{2}\int \frac{b(\theta)}{d(\theta)} d\theta\right\} \frac{\sqrt{a(\theta)b(\theta)}}{d(\theta)}, \quad (10)$$

where g is a continuously differentiable function, $a(\theta)$ and $b(\theta)$ are defined in (7) and (8), respectively, and

$$d(\theta) = \sum_{i=1}^{r} \frac{h_i \lambda_i}{\theta^{h_i+1}}.$$

Remark 3. If we take $g(x) = x^{-\frac{3}{2}}$, the priors $\pi_M(\vartheta)$ is then simplified to

$$\pi_M(\vartheta) = \eta_0^{-\frac{3}{2}} \sigma^{-1} \frac{\sqrt{a(\theta)b(\theta)}}{d(\theta)}. \quad (11)$$

Furthermore, the simultaneous marginal probability matching prior $\pi_M(\vartheta)$ is also the joint probability matching prior, since the parametric functions $\phi_j(\vartheta)$, $j = 1, 2$, satisfy the conditions given in Theorem 1 of [7].

Remark 4. It can be verified that the Jeffreys prior (6) and the reference priors (π_{R_1}, π_{R_2} and π_{R_3}) are not probability matching priors.

4. POSTERIOR ANALYSIS

It is to be remarked that the noninformative priors obtained in Section 3 are all improper and can be rewritten in the following unified form

$$\pi_U(\eta_0, \theta, \sigma) \propto \frac{\pi(\theta)}{\eta_0^p \sigma^q}, \quad (12)$$

for certain constants p and q, where $\pi(\theta)$ is the marginal prior for θ. In this section, we will investigate a significant issue that whether these improper priors will result in proper posterior distributions. The results are summarized in the following three theorems.

Theorem 4.1. *The posterior distribution of (η_0, θ, σ) is proper under the Jeffreys prior π_J in (6).*

Theorem 4.2. *The posterior distributions of (η_0, θ, σ) are improper based on the reference priors π_{R_1} and π_{R_2}.*

Theorem 4.3. *If $N \geq 2$, then based on the priors π_{R_3} and π_{R_M}, the posterior distributions of (η_0, θ, σ) are proper.*

In the following we consider a Monte Carlo procedure to generate samples from the proper posterior distribution with respect to the unified prior (12). Note that the marginal density of η_0 and θ cannot be written in a closed form, so we use a Metropolis random walk algorithm to generate samples from the joint marginal posterior distribution of η_0 and θ. The procedure is stated as follows:

Step 1: Under the prior $\pi_U(\eta_0, \theta, \sigma)$, the joint marginal posterior distribution of η_0 and θ is given by

$$\pi_U(\eta_0, \theta | \boldsymbol{y}) \propto \frac{\pi(\theta)}{\eta_0^p \psi^{\frac{N}{2} - q + 1}}.$$

Step 2: Given η_0 and θ, the conditional posterior distribution of σ, $\pi(\sigma | \eta_0, \theta, \boldsymbol{y})$, follows a gamma distribution with shape parameter $(\frac{N}{2} - q + 1)$ and scale parameter ψ.

The Metropolis random walk algorithm in Step 1 can be implemented by using the function *rwmetrop* in the *LearnBayes* package of R software. Here we make a logarithm transformation for the parameters (η_0, θ) since they are positive with $\theta > 1$. Besides, we use the function *laplace* in the *LearnBayes* package to achieve some reasonable initial values, such as the posterior mode and the associated variance-covariance matrix of the alternative posterior distribution. The R package, *LearnBayes*, is available on the CRAN site, and detailed guidance on this package can be found in the monograph by Albert [1]. A written R code is also available from the corresponding author upon request.

5. SIMULATION STUDY

To assess the performance of the Bayesian estimators based on the priors π_J, π_{R_3} and π_M, a small simulation experiment is carried out to compare with maximum likelihood estimator (MLE) in terms of squared root of mean squared error (SRMSE) and frequentist coverage probability for different parameter values and sample sizes. In this experiment, we assume that the degradation characteristic $y(t)$ ($y(0) = 0$) follows an IG process with temperature as the stress variable, and the Arrhenius model is assumed between the parameter η and the temperature. The degradation data are collected under three temperature levels,

$$S_1 = 83^{\circ}\text{C},\ S_2 = 133^{\circ}\text{C},\ S_3 = 173^{\circ}\text{C}.$$

The maximum test duration allowed for each unit is 2000h and the number of measurements is 4 (i.e., at 100h, 400h, 1000h and 2000h, respectively).

For simplicity we only consider two different cases for the parameters (η_0, θ, σ), which are

$$\text{Case A} : \eta_0 = 1.93 \times 10^{-4}, \theta = 3.6765, \sigma = 7.29 \times 10^{-2},$$
$$\text{Case B} : \eta_0 = 2.68 \times 10^{-2}, \theta = 1.1969, \sigma = 8.36 \times 10^{-3}.$$

For Cases A and B, the product is assumed to fail when $y(t)$ exceeds 5 and 50 under the operating temperature 50°C, that is, $\nu = 5$ and 50. A direct calculation yields that the true values of MTTF_0 are around 25906.74h and 1867.275h, respectively.

Under the setup above, we use the algorithm in Section 4 to calculate the Bayesian estimators of the parameters for different sample sizes (n_1, n_2, n_3), including the

Table 1. SRMSEs of $\widehat{MTTF}_0$, Bayesian estimators and MLE of the parameters (η_0, θ, σ) for Case A.

(n_1, n_2, n_3)	Parameters	MLE	Posterior Mean			Posterior Median			Posterior Mode		
			π_J	π_{R_3}	π_M	π_J	π_{R_3}	π_M	π_J	π_{R_3}	π_M
(1,1,1)	$\eta_0 \times 10^{-7}$	8.8527	8.8554	8.8581	8.8503	8.8571	8.8562	8.8571	9.4366	9.5003	9.5133
	$\theta \times 10^{-2}$	1.1599	1.1606	1.1608	1.1595	1.1607	1.1598	1.1604	1.2393	1.2381	1.2503
	$\sigma \times 10^{-2}$	7.3194	7.3197	5.5956	5.5944	6.7266	5.0923	5.0925	8.9351	7.5499	7.3644
	$\mathrm{MTTF}_0 \times 10^2$	1.1885	1.1888	1.1891	**1.1881**	1.1891	**1.1889**	1.1891	**1.2669**	1.2750	1.2774
		$(0.948)^\dagger$	(0.948)	(0.949)	(**0.948**)	(0.949)	(**0.948**)	(0.949)	(**1.007**)	(1.012)	(1.017)
(3,3,3)	$\eta_0 \times 10^{7}$	5.1703	5.1707	5.1697	5.1741	5.1733	5.1731	5.1759	5.6724	5.6512	5.5778
	$\theta \times 10^{-2}$	0.6753	0.6753	0.6752	0.6755	0.6754	0.6756	0.6757	0.7367	0.7403	0.7269
	$\sigma \times 10^{-2}$	2.2678	2.2679	2.0220	2.0216	2.1778	1.9585	1.9575	3.0932	2.7031	2.8132
	$\mathrm{MTTF}_0 \times 10^2$	0.6939	0.6939	**0.6937**	0.6944	0.6943	**0.6942**	0.6946	0.7612	0.7584	**0.7486**
		(0.555)	(0.554)	(**0.554**)	(0.555)	(0.555)	(**0.555**)	(0.555)	(0.611)	(0.608)	(**0.598**)
(5,5,5)	$\eta_0 \times 10^{-7}$	3.9466	3.9492	3.9451	3.9472	3.9513	3.9462	3.9475	4.2981	4.3311	4.2955
	$\theta \times 10^{-2}$	0.5186	0.5191	0.5186	0.5188	0.5192	0.5187	0.5188	0.5681	0.5685	0.5643
	$\sigma \times 10^{-2}$	1.5726	1.5729	1.4604	1.4603	1.5315	1.4320	1.4319	2.1280	2.0210	2.0593
	$\mathrm{MTTF}_0 \times 10^2$	0.5297	0.5301	**0.5295**	0.5298	0.5303	**0.5296**	0.5298	0.5768	0.5812	**0.5766**
		(0.424)	(0.425)	(**0.424**)	(0.424)	(0.425)	(**0.424**)	(0.424)	(0.461)	(0.464)	(**0.461**)
(10,10,10)	$\eta_0 \times 10^{-7}$	2.8621	2.8638	2.8606	2.8617	2.8646	2.8607	2.8617	3.0964	3.1056	3.1272
	$\theta \times 10^{-2}$	0.3786	0.3787	0.3786	0.3786	0.3.789	0.3785	0.3786	0.4087	0.4105	0.4120
	$\sigma \times 10^{-2}$	1.0280	1.0279	0.9864	0.9866	1.0127	0.9760	0.9757	1.4201	1.4010	1.3856
	$\mathrm{MTTF}_0 \times 10^2$	0.3841	0.3843	**0.3839**	0.3841	0.3844	**0.3839**	0.3841	**0.4156**	0.4168	0.4197
		(0.305)	(0.305)	(**0.304**)	(0.305)	(0.305)	(**0.304**)	(0.305)	(**0.332**)	(0.333)	(0.336)
(20,20,20)	$\eta_0 \times 10^{-7}$	2.0187	2.0194	2.0190	2.0207	2.0202	2.0196	2.0212	2.1988	2.2300	2.2507
	$\theta \times 10^{-2}$	0.2653	0.2654	0.2653	0.2655	0.2656	0.2655	0.2655	0.2846	0.2936	0.2949
	$\sigma \times 10^{-2}$	0.6902	0.6902	0.6755	0.6755	0.6847	0.6720	0.6719	0.9536	0.9538	0.9539
	$\mathrm{MTTF}_0 \times 10^2$	0.2710	0.2711	**0.2710**	0.2712	0.2712	**0.2711**	0.2713	**0.2951**	0.2993	0.3021
		(0.216)	(0.216)	(**0.216**)	(0.216)	(0.216)	(**0.216**)	(0.217)	(**0.234**)	(0.238)	(0.241)

† The absolute biases of $\widehat{\mathrm{MTTF}}_0$

posterior mean, posterior median and posterior mode. The MLE of (η_0, θ, σ) are also computed, in which $\hat{\theta}_{ML}$ can be obtained by maximizing the profile log-likelihood function $\mathcal{L}(\theta|\boldsymbol{y}) \propto -(N/2)\log\{-\beta_\theta^2/(4\alpha_\theta) + \gamma\}$ through a one-dimensional search, where α_θ, β_θ and γ are defined in (16). Moreover, substitute $\hat{\theta}_{ML}$ into $\hat{\eta_0}(\theta) = 2\alpha_\theta/\beta_\theta$, and $(\hat{\eta_0}_{ML}, \hat{\theta}_{ML})$ into $\hat{\sigma}(\eta_0, \theta) = N/(2(\alpha_\theta/\eta_0^2 - \beta_\theta/\eta_0 + \gamma))$, we obtain the MLE for η_0 and σ, as $\hat{\eta_0}_{ML} = \hat{\eta_0}(\hat{\theta}_{ML})$ and $\hat{\sigma}_{ML} = \hat{\sigma}(\hat{\eta_0}_{ML}, \hat{\theta}_{ML})$, respectively. 5000 replications are generated for each simulation and the SRMSEs are computed for the parameters (η_0, θ, σ) and MTTF_0 under the Cases A and B. The simulated results are listed in Tables 1 and 2, which also contain the absolute biases (ABs) of the MLE and Bayesian estimators of the MTTF_0.

It can be observed from Tables 1 and 2 that the RSMSEs of all the parameter estimates become smaller and closer as the sample size increases. Furthermore, the other points are also clear from the numerical results:

- The posterior mean and posterior median perform in a similar manner for both cases, which are consistently superior to the posterior mode and so is MLE since their RSMSEs are much smaller.
- Using the posterior mean and posterior median, for estimating η_0 and θ the Bayesian estimators under the three priors are almost the same in term of RSMSE, but the priors π_{R_3} and π_M yield better estimate of σ.
- The Bayesian estimators of the MTTF_0 under the prior π_{R_3} perform better than the MLE and the Bayesian estimators under the priors π_J and π_M in terms of AB and RSMSE when the posterior median is employed.

On the other hand, we want to compare the frequentist coverage probabilities for different Bayesian estimators under the priors π_J, π_{R_3} and π_M. Let $\eta_0^{\pi_J}(\alpha; \boldsymbol{y})$, $\theta^{\pi_J}(\alpha; \boldsymbol{y})$ and $\sigma^{\pi_J}(\alpha; \boldsymbol{y})$ be the posterior α-quantiles of η_0, θ and σ based on the Jeffreys prior π_J, respectively. Then the frequentist coverage probability of $\eta_0^{\pi_J}(\alpha; \boldsymbol{y})$ can be expressed as

$$Q^{\pi_J}(\alpha, \eta_0) = \mathrm{P}_\vartheta(0 < \eta_0 < \eta_0^{\pi_J}(\alpha; \boldsymbol{y})).$$

Similarly, the frequentist coverage probabilities of $\theta^{\pi_J}(\alpha; \boldsymbol{y})$ and $\sigma^{\pi_J}(\alpha; \boldsymbol{y})$ can also be defined, which are denoted by $Q^{\pi_J}(\alpha, \theta)$ and $Q^{\pi_J}(\alpha, \sigma)$, respectively. Replacing the superscript π_J by π_{R_3} and π_M means that these quantities are computed based on the reference prior π_{R_3} and matching prior π_M, respectively. For Cases A and B, the numerical values of the frequentist coverage probabilities of 95% credible intervals under the three priors are shown in Tables 3 and 4, respectively.

Table 2. SRMSEs of $\widehat{MTTF}_0$, Bayesian estimators and MLE of the parameters (η_0, θ, σ) for Case B.

(n_1, n_2, n_3)	Parameters	MLE	Posterior Mean			Posterior Median			Posterior Mode		
			π_J	π_{R_3}	π_M	π_J	π_{R_3}	π_M	π_J	π_{R_3}	π_M
(1,1,1)	$\eta_0 \times 10^{-3}$	3.0351	2.6718	2.6068	2.6085	2.7763	2.7273	2.7325	3.4098	3.4956	3.5188
	$\theta \times 10^{-2}$	9.3321	8.7488	8.7045	8.7065	8.8249	8.7309	8.7437	10.709	11.076	11.061
	$\sigma \times 10^{-3}$	8.2947	8.3378	6.3637	6.3646	7.6566	5.7797	5.7828	11.661	10.091	10.133
	$\mathrm{MTTF}_0 \times 10^2$	2.1651	1.9989	**1.9611**	1.9636	2.0603	**2.0389**	2.0422	**2.4778**	2.5648	2.5540
		(1.712)†	(1.566)	(**1.528**)	(1.532)	(1.622)	(**1.598**)	(1.601)	(**1.947**)	(2.003)	(2.007)
(3,3,3)	$\eta_0 \times 10^{-3}$	1.7553	1.7426	1.7370	1.7403	1.7486	1.7427	1.7451	2.0399	2.0764	2.0886
	$\theta \times 10^{-2}$	5.3195	5.2905	5.2748	5.2845	5.3103	5.2903	5.2978	6.2020	6.2700	6.2887
	$\sigma \times 10^{-3}$	2.6538	2.6548	2.3562	2.3583	2.5466	2.2777	2.2793	3.7875	3.4562	3.5348
	$\mathrm{MTTF}_0 \times 10^2$	1.2292	1.2147	**1.2111**	1.2129	1.2260	**1.2227**	1.2243	**1.4234**	1.4407	1.4505
		(0.978)	(0.970)	(**0.967**)	(0.968)	(0.977)	(**0.973**)	(0.975)	(**1.104**)	(1.114)	(1.128)
(5,5,5)	$\eta_0 \times 10^{-3}$	1.3680	1.3704	1.3701	1.3705	1.3684	1.3674	1.3677	1.5096	1.5187	1.5024
	$\theta \times 10^{-2}$	4.1343	4.1346	4.1313	4.1346	4.1378	4.1301	4.1338	4.6181	4.6344	4.5962
	$\sigma \times 10^{-3}$	1.8078	1.8080	1.6770	1.6755	1.7591	1.6431	1.6417	2.5495	2.4449	2.4918
	$\mathrm{MTTF}_0 \times 10^2$	0.9519	0.9492	**0.9485**	0.9489	0.9520	**0.9511**	0.9517	1.0635	1.0667	**1.0577**
		(0.753)	(0.752)	(**0.751**)	(0.752)	(0.753)	(**0.752**)	(0.753)	(0.841)	(0.832)	(**0.826**)
(10,10,10)	$\eta_0 \times 10^{-3}$	0.9725	0.9746	0.9747	0.9764	0.9735	0.9717	0.9743	1.0541	1.0527	1.0513
	$\theta \times 10^{-2}$	2.9798	2.9807	2.9802	2.9854	2.9802	2.9757	2.9844	3.2474	3.2586	3.2244
	$\sigma \times 10^{-2}$	1.1279	1.1278	1.0849	1.0852	1.1118	1.0750	1.0754	1.6155	1.4871	1.5698
	$\mathrm{MTTF}_0 \times 10^2$	0.6745	0.6741	**0.6740**	0.6751	0.6748	**0.6736**	0.6754	0.7404	0.7410	**0.7322**
		(0.535)	(0.535)	(**0.534**)	(0.536)	(0.535)	(**0.534**)	(0.536)	(0.584)	(0.586)	(**0.581**)
(20,20,20)	$\eta_0 \times 10^{-3}$	0.6992	0.6999	0.6990	0.7005	0.7001	0.6989	0.7004	0.7646	0.7604	0.7435
	$\theta \times 10^{-2}$	2.1223	2.1247	2.1212	2.1259	2.1238	2.1201	2.1262	2.3389	2.3163	2.2805
	$\sigma \times 10^{-3}$	0.8411	0.8407	0.8268	0.8266	0.8352	0.8232	0.8231	1.1321	1.1010	1.1435
	$\mathrm{MTTF}_0 \times 10^2$	0.4877	0.4876	**0.4875**	0.4879	0.4882	**0.4874**	0.4884	0.5379	0.5326	**0.5227**
		(0.394)	(0.393)	(**0.393**)	(0.394)	(0.394)	(**0.394**)	(0.394)	(0.426)	(0.433)	(**0.422**)

† The absolute biases of $\widehat{\mathrm{MTTF}}_0$

Table 3. 95% coverage probabilities of Bayesian estimators for Case A

(n_1, n_2, n_3)	η_0			θ			σ		
	π_J	π_{R_3}	π_M	π_J	π_{R_3}	π_M	π_J	π_{R_3}	π_M
(1, 1, 1)	0.9318	0.9520	0.9524	0.9366	0.9534	0.9536	0.9772	0.9522	0.9522
(3, 3, 3)	0.9460	0.9506	0.9512	0.9420	0.9470	0.9468	0.9682	0.9482	0.9482
(5, 5, 5)	0.9482	0.9516	0.9522	0.9480	0.9514	0.9508	0.9650	0.9498	0.9498
(10, 10, 10)	0.9496	0.9508	0.9514	0.9474	0.9489	0.9486	0.9626	0.9492	0.9502
(20, 20, 20)	0.9492	0.9498	0.9496	0.9482	0.9496	0.9494	0.9588	0.9506	0.9502

Table 4. 95% coverage probabilities of Bayesian estimators for Case B

(n_1, n_2, n_3)	η_0			θ			σ		
	π_J	π_{R_3}	π_M	π_J	π_{R_3}	π_M	π_J	π_{R_3}	π_M
(1, 1, 1)	0.9242	0.9426	0.9424	0.9330	0.9606	0.9618	0.9817	0.9531	0.9532
(3, 3, 3)	0.9394	0.9478	0.9450	0.9366	0.9540	0.9524	0.9724	0.9498	0.9488
(5, 5, 5)	0.9446	0.9498	0.9486	0.9472	0.9516	0.9508	0.9690	0.9508	0.9512
(10, 10, 10)	0.9480	0.9504	0.9498	0.9546	0.9510	0.9504	0.9614	0.9510	0.9506
(20, 20, 20)	0.9488	0.9494	0.9496	0.9520	0.9510	0.9508	0.9602	0.9504	0.9504

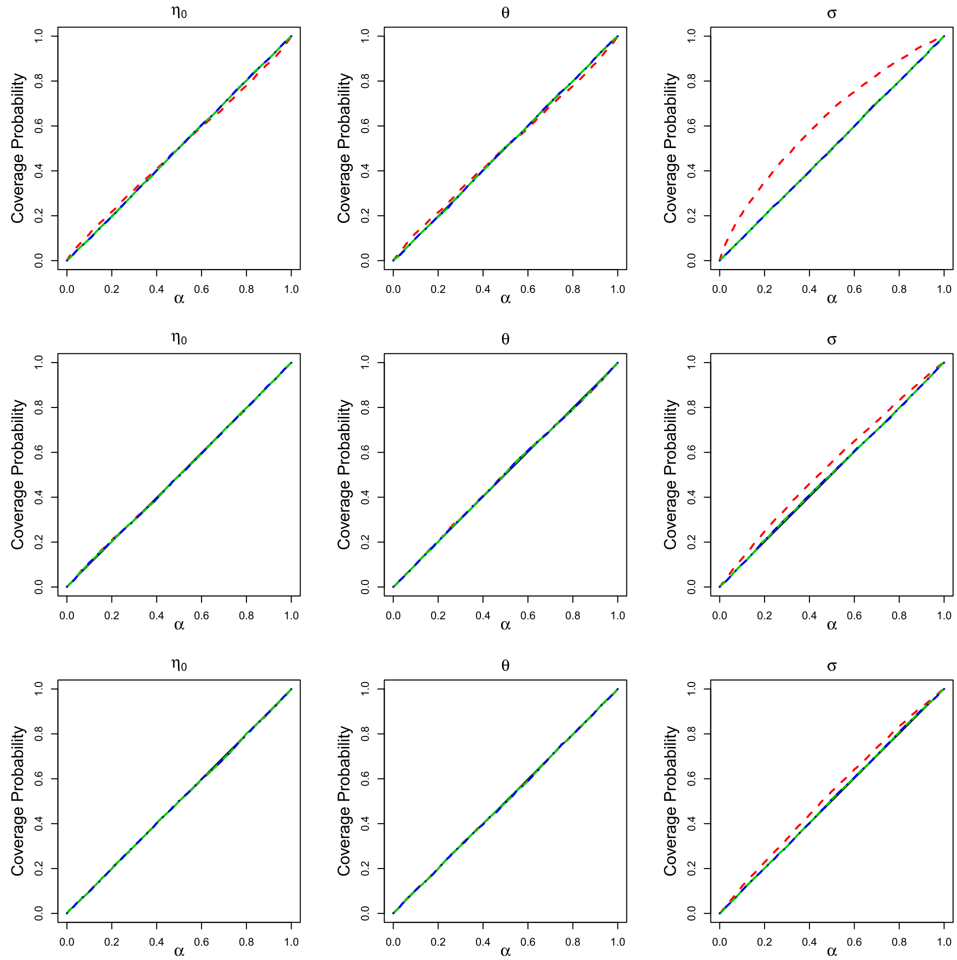

Figure 1. The coverage probabilities of (η_0, σ, θ) under the priors π_J (- - - - -), π_{R_3} (———) and π_M (-·-·-·-) for Case A. The upper, middle and lower parts correspond to $(n_1, n_2, n_3) = (1, 1, 1)$, $(10, 10, 10)$ and $(20, 20, 20)$, respectively.

According to the results in Tables 3 and 4, we find that the coverage probabilities are much close to 0.95 when the sample size increases, and note that the Bayesian estimators of (η_0, θ, σ) under the priors π_{R_3} and π_M perform better than the Jeffreys prior π_J, since most of its coverage probabilities are much more close to 0.95 even for small sample sizes.

Another way of making comparisons is to present the coverage probabilities. Here we make graphs of the coverage probabilities for (η_0, θ, σ) with respect to nominal confidence levels based on the priors π_J, π_{R_3} and π_M. From Figures 1 and 2, we can see that the performance of the reference prior π_{R_3} and that of the matching prior π_M are very similar. However, the Bayesian estimator of σ under the Jeffreys prior π_J behave unsatisfactory in meeting the target coverage probabilities.

6. REAL DATA ANALYSIS

In this section, we apply the objective Bayesian analysis to the degradation data from the carbon-film-resistor problem reported in [15]. The data can be found in Table C.3 of [15]. Note that the resistance value of the carbon-film resistors will increase over time, which means that the performance of the product is on the decline. In this example, the resistors were exposed to three different levels of temperature (83°C, 133°C and 173°C) to accelerate the degradation process. Also, the percent increase in resistance for each unit was measured at $t_1 = 452$, $t_2 = 1030, t_3 = 4341$ and $t_4 = 8084$ (in hours). The use condition S_0 is specified as 50°C and the critical value is taken to be $\nu = 5$.

We note that the degradation path of each unit has independent positive increments, except for the unit number 27. So we delete them and model the degradation behavior using the IG process model (1) in this application. Similar to [21] and [30], we adopt the Arrhenius model to characterize the relationship between the parameter η and the temperature, i.e., $\log(\eta_i) = v_0 + v_1/(273 + S_i)$, $i = 0, 1, 2, 3$.

Here three objective priors π_J, π_{R_3} and π_M are used. Posterior means of the parameters (η_0, θ, σ) and their 95% credible intervals can be obtained directly using the algorithm

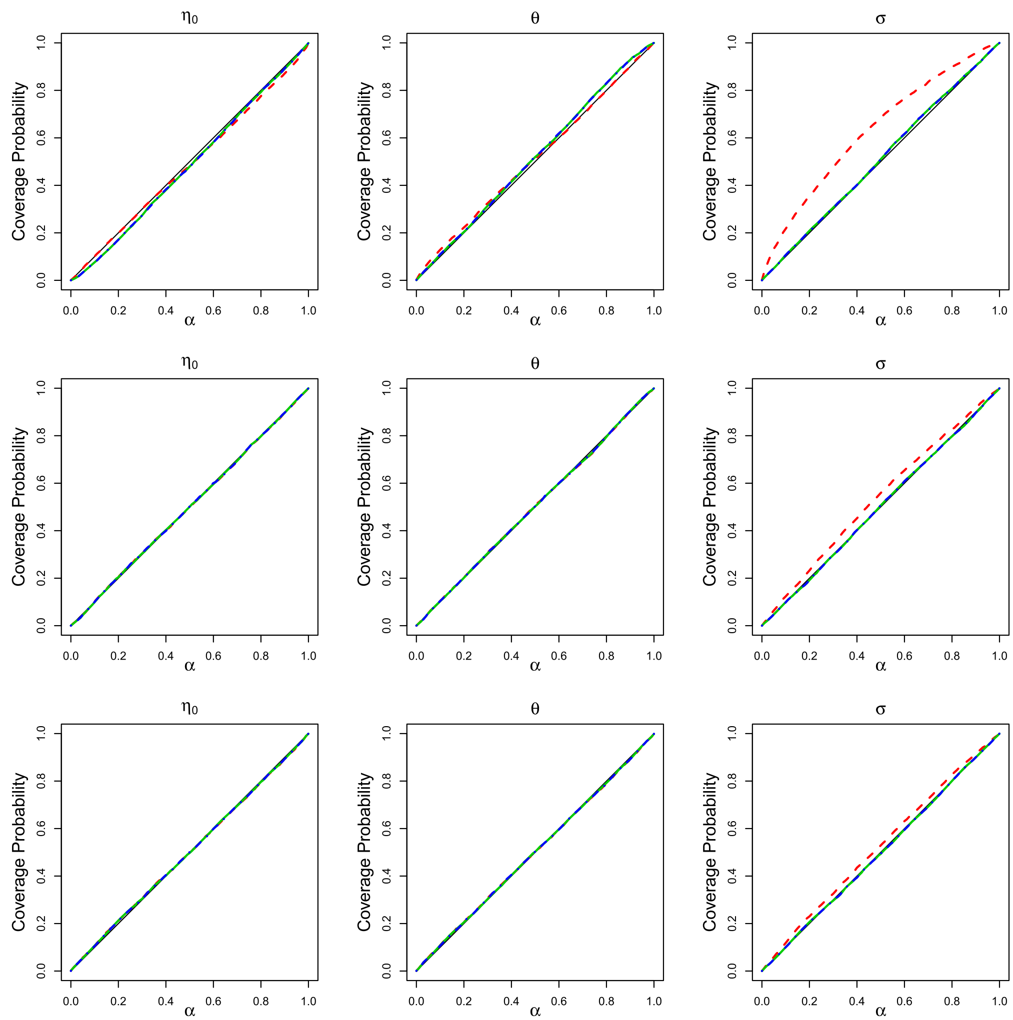

Figure 2. The coverage probabilities of (η_0, σ, θ) under the priors π_J (- - - -), π_{R_3} (——) and π_M (-·-·-) for Case B. The upper, middle and lower parts correspond to $(n_1, n_2, n_3) = (1, 1, 1)$, $(10, 10, 10)$ and $(20, 20, 20)$, respectively.

Table 5. Posterior means and 95% credible intervals (within parentheses) of parameters

Parameters	π_J	π_{R_3}	π_M
$\eta_0 \times 10^{-5}$	2.6563	2.6960	2.6841
	(1.484,4.473)	(1.482,4.559)	(1.448,4.592)
θ	3.0503	3.0509	3.0661
	(2.179,4.448)	(2.162,4.480)	(2.164,4.599)
$\sigma \times 10^{-8}$	5.4893	5.3946	5.3927
	(4.158,7.034)	(4.064,6.911)	(4.068,6.926)
$\mathrm{MTTF}_0 \times 10^5$	1.8847	1.8571	1.8652
	(1.121,3.337)	(1.101,3.338)	(1.092,3.454)

given in Section 4, in which the scale parameter involved in Step 1 is specified as 2 and the acceptance rate is about 0.29. The results are shown in Table 5 along with the estimates for MTTF at S_0. It can be observed from Table 5 that all the Bayesian estimates are nearly the same.

To evaluate the effectiveness of the Metropolis random walk algorithm, we show in Figure 3(a)-3(c) the associated diagnostics, including the posterior density, the trace, the running mean and the autocorrelation function (ACF) plot, for drawing samples of the parameters (η_0, θ, σ) under the priors π_J, π_{R_3} and π_M, which indicate the convergence is satisfied.

7. CONCLUDING REMARKS

In this paper, we propose an objective Bayesian analysis method for CSADTs based on the IG process. The Jeffreys prior, reference priors and probability matching priors are developed for such model. The properties of these priors and resulting posteriors are investigated. According to the simulation study, the reference prior π_{R_3} is recommended as the default priors in practice since it can lead to more better results for estimating MTTF_0 in most cases. Finally,

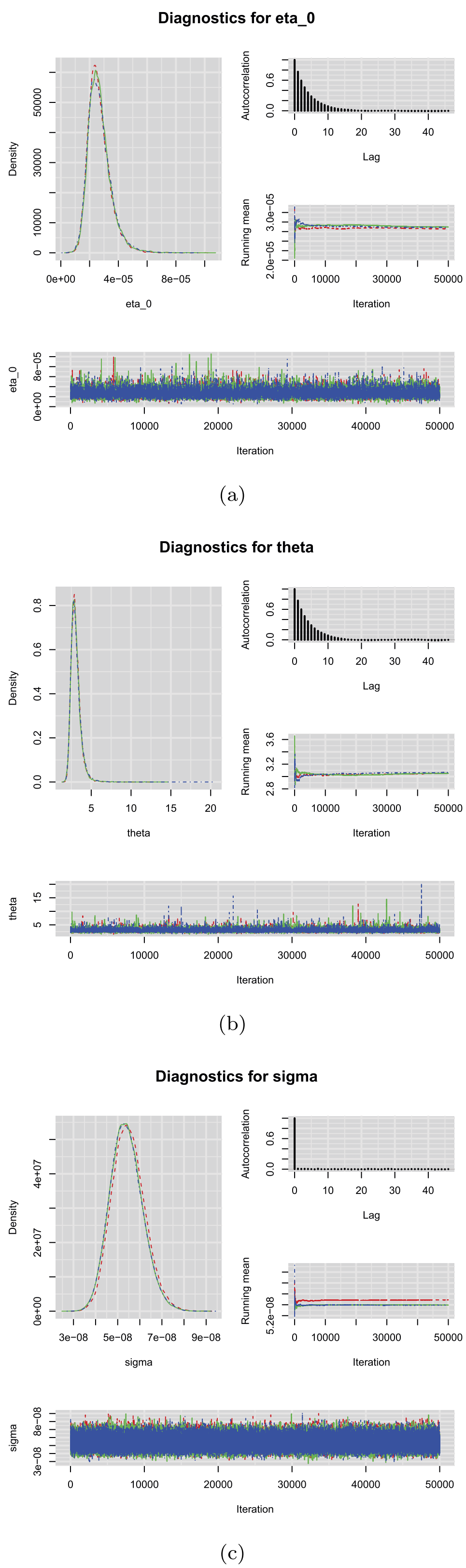

Figure 3. MCMC diagnostic plots: (a)-(c) for parameters (η_0, θ, σ) via the priors π_J (- - - - -), π_{R_3} (———) and π_M (-·-·-·-).

we apply the method to a real data set, and obtain the Bayesian estimates of the product's MTTF_0.

APPENDIX A. PROOFS

In this section we present detailed proofs of the theoretical results obtained in Sections 3 and 4.

A.1 Proof of Theorem 3.1

Proof. By (5), the log-likelihood function of ϑ, up to a constant, is

(13)
$$\mathcal{L}(\vartheta|\boldsymbol{y}) = \sum_{i=1}^{r}\sum_{j=1}^{n_i}\sum_{k=1}^{m_{ij}} \left\{ \frac{\log\sigma}{2} - \frac{\sigma(\Delta y_{ijk} - \eta_0\theta^{h_i}\lambda_{ijk})^2}{2\eta_0^2\theta^{2h_i}\Delta y_{ijk}} \right\}.$$

Consequently, the second partial derivatives of the log-likelihood function (13) with respect to the three parameters are given, respectively, by

$$\frac{\partial^2\mathcal{L}(\vartheta|\boldsymbol{y})}{\partial\eta_0^2} = -\sum_{i=1}^{r}\sum_{j=1}^{n_i}\sum_{k=1}^{m_{ij}} \frac{\sigma(3\Delta y_{ijk} - 2\eta_0\theta^{h_i}\lambda_{ijk})}{\eta_0^4\theta^{2h_i}},$$

$$\frac{\partial^2\mathcal{L}(\vartheta|\boldsymbol{y})}{\partial\eta_0\partial\theta} = -\sum_{i=1}^{r}\sum_{j=1}^{n_i}\sum_{k=1}^{m_{ij}} \frac{\sigma(2\Delta y_{ijk}h_i - \eta_0 h_i\theta^{h_i}\lambda_{ijk})}{\eta_0^3\theta^{2h_i+1}},$$

$$\frac{\partial^2\mathcal{L}(\vartheta|\boldsymbol{y})}{\partial\eta_0\partial\sigma} = -\sum_{i=1}^{r}\sum_{j=1}^{n_i}\sum_{k=1}^{m_{ij}} \frac{\eta_0\theta^{h_i}\lambda_{ijk} - \Delta y_{ijk}}{\eta_0^3\theta^{2h_i}},$$

$$\frac{\partial^2\mathcal{L}(\vartheta|\boldsymbol{y})}{\partial\theta\partial\sigma} = -\sum_{i=1}^{r}\sum_{j=1}^{n_i}\sum_{k=1}^{m_{ij}} \frac{\eta_0 h_i\theta^{h_i}\lambda_{ijk} - \Delta y_{ijk}h_i}{\eta_0^2\theta^{2h_i+1}},$$

$$\frac{\partial^2\mathcal{L}(\vartheta|\boldsymbol{y})}{\partial\theta^2} = -\sum_{i=1}^{r}\sum_{j=1}^{n_i}\sum_{k=1}^{m_{ij}} \frac{\sigma[\Delta y_{ijk}h_i(2h_i+1) - \eta_0 h_i^2\theta^{h_i}\lambda_{ijk} - \eta_0 h_i\theta^{h_i}\lambda_{ijk}]}{\eta_0^2\theta^{2h_i+2}},$$

$$\frac{\partial^2\mathcal{L}(\vartheta|\boldsymbol{y})}{\partial\sigma^2} = -\sum_{i=1}^{r}\sum_{j=1}^{n_i}\sum_{k=1}^{m_{ij}} \frac{1}{2\sigma^2}.$$

Since each $\Delta y_{ijk} \sim \mathcal{IG}(\eta_0\theta^{h_i}\lambda_{ijk}, \sigma\lambda_{ijk}^2)$, we have $\mathrm{E}(\Delta y_{ijk}) = \eta_0\theta^{h_i}\lambda_{ijk}$. Then the result of Theorem 3.1 is clear. $\square$

A.2 Proof of Theorem 3.2

Proof. We only give the proof for the group ordering $\{\eta_0, \sigma, \theta\}$, in that the other cases can be derived in a similar way. For the group ordering $\{\eta_0, \sigma, \theta\}$, the inverse of the

Fisher information matrix is given by

$$(14)\quad S = H^{-1}(\vartheta) = \begin{pmatrix} \frac{\eta_0^3 b(\theta)}{\sigma a(\theta)} & 0 & -\frac{\eta_0^2}{\sigma a(\theta)} \sum_{i=1}^r \frac{h_i\lambda_i}{\theta^{h_i+1}} \\ 0 & \frac{2\sigma^2}{N} & 0 \\ -\frac{\eta_0^2}{\sigma a(\theta)} \sum_{i=1}^r \frac{h_i\lambda_i}{\theta^{h_i+1}} & 0 & \frac{\eta_0}{\sigma a(\theta)} \sum_{i=1}^r \frac{\lambda_i}{\theta^{h_i}} \end{pmatrix},$$

where $a(\theta)$ is defined in (7), and $b(\theta) = \sum_{i=1}^r \frac{h_i^2\lambda_i}{\theta^{h_i+2}}$. Following the notations of [5], it is readily to obtain from (14) that

$$h_1 = \frac{\sigma a(\theta)}{\eta_0^3 b(\theta)}, \quad h_2 = \frac{N}{2\sigma^2}, \quad h_3 = \frac{\sigma b(\theta)}{\eta_0}.$$

Moreover, we choose the following compact sets $\Omega_l = [c_{1l}, d_{1l}]\times[c_{2l}, d_{2l}]\times[c_{3l}, d_{3l}]$ for (η_0, σ, θ), such that $c_{1l}, c_{2l} \to 0$, $c_{3l} \to 1$ and $d_{1l}, d_{2l}, d_{3l} \to +\infty$, as $l \to \infty$. Then

$$\pi_3^l(\theta|\eta_0, \sigma) = \frac{|h_3|^{1/2}\mathbf{1}_{[c_{3l},d_{3l}]}(\theta)}{\int_{c_{3l}}^{d_{3l}} |h_3|^{1/2}\mathrm{d}\theta} = \frac{\sqrt{b(\theta)}}{c_1(l)}\mathbf{1}_{[d_{3l},e_{3l}]}(\theta),$$

where $c_1(l) = \int_{c_{3l}}^{d_{3l}} \sqrt{b(\theta)}\mathrm{d}\theta$ is a constant, and $\mathbf{1}_A(\cdot)$ denotes the indicator function on the set A. Also we have

$$\begin{aligned} \mathrm{E}_2^l[\log(|h_2|)|\eta_0, \sigma] &= \int_{c_{3l}}^{d_{3l}} \log(|h_2|)\pi_3^l(\theta|\eta_0, \sigma)\mathrm{d}\theta \\ &= \int_{c_{3l}}^{d_{3l}} \log\left(\frac{N}{2\sigma^2}\right)\frac{\sqrt{b(\theta)}}{c_1(l)}\mathrm{d}\theta \\ &= \log\left(\frac{N}{2\sigma^2}\right). \end{aligned}$$

Therefore,

$$\begin{aligned} &\pi_2^l(\sigma, \theta|\eta_0) \\ &\quad= \frac{\pi_3^l(\theta|\eta_0, \sigma)\exp\{\frac{1}{2}\mathrm{E}_2^l[\log(|h_2|)|\eta_0, \sigma]\}\mathbf{1}_{[c_{2l},d_{2l}]}(\sigma)}{\int_{c_{2l}}^{d_{2l}} \exp\{\frac{1}{2}\mathrm{E}_2^l[\log(|h_2|)|\eta_0, \sigma]\}\mathrm{d}\sigma} \\ &\quad= \pi_3^l(\theta|\eta_0, \sigma)\frac{1}{\sigma\log(\frac{d_{2l}}{c_{2l}})}\mathbf{1}_{[c_{2l},d_{2l}]}(\sigma). \end{aligned}$$

Note that

$$\begin{aligned} \mathrm{E}_1^l[\log(|h_1|)|\eta_0] &= \int_{c_{3l}}^{d_{3l}}\int_{c_{2l}}^{d_{2l}} \log(|h_1|)\pi_2^l(\sigma, \theta|\eta_0)\mathrm{d}\sigma\mathrm{d}\theta \\ [3pt] &= \frac{1}{2}\log(c_{2l}d_{2l}) + c_2(l) - 3\log(\eta_0), \end{aligned}$$

where

$$c_2(l) = \frac{1}{c_1(l)}\int_{c_{3l}}^{d_{3l}} \sqrt{b(\theta)}\log\left[\frac{a(\theta)}{b(\theta)}\right]\mathrm{d}\theta,$$

it follows that

$$\begin{aligned} &\pi_1^l(\sigma, \eta_0, \theta) \\ &\quad= \frac{\pi_2^l(\sigma, \theta|\eta_0)\exp\{\mathrm{E}_1^l[\log(|h_1|)|\eta_0]\}\mathbf{1}_{[c_{1l},d_{1l}]}(\eta_0)}{\int_{c_{1l}}^{d_{1l}} \exp\{\mathrm{E}_1^l[\log(|h_1|)|\eta_0]\}\mathrm{d}\eta_0} \\ &\quad= \eta_0^{-\frac{3}{2}}\sigma^{-1}\sqrt{b(\theta)}\frac{\sqrt{c_{1l}d_{1l}}}{2(\sqrt{d_{1l}}-\sqrt{c_{1l}})c_1(l)\log(\frac{d_{2l}}{c_{2l}})}\mathbf{1}_{\Omega_l}(\sigma, \eta_0, \theta). \end{aligned}$$

Therefore, the reference prior for the group $\{\eta_0, \sigma, \theta\}$ is given by

$$\pi_{R_1}(\eta_0, \sigma, \theta) = \lim_{l\to\infty}\frac{\pi_1^l(\eta_0, \sigma, \theta)}{\pi_1^l(1, 1, 2)} \propto \eta_0^{-\frac{3}{2}}\sigma^{-1}\sqrt{b(\theta)}. \qquad \square$$

A.3 Proof of Theorem 4.1

Proof. Let $L(\vartheta|\boldsymbol{y})$ denote the likelihood function of ϑ based on $\boldsymbol{y}$. Then the posterior $\pi_J(\eta_0, \theta, \sigma|\boldsymbol{y})$ with respect to the Jeffreys prior, up to a constant, can be written as

$$\begin{aligned} (15)\quad &\pi_J(\eta_0, \theta, \sigma|\boldsymbol{y}) \propto L(\vartheta|\boldsymbol{y})\pi_J(\eta_0, \theta, \sigma) \\ &\quad= \eta_0^{-2}\sqrt{a(\theta)}\prod_{i=1}^r\prod_{j=1}^{n_i}\prod_{k=1}^{m_{ij}}\sqrt{\frac{\sigma\lambda_{ijk}^2}{2\pi y_{ijk}^3}}\cdot \\ &\qquad \exp\left\{-\frac{\sigma(y_{ijk}-\eta_0\theta^{h_i}\lambda_{ijk})^2}{2\eta_0^2\theta^{2h_i}y_{ijk}}\right\} \\ &\quad\propto \sqrt{a(\theta)}\eta_0^{-2}\sigma^{\frac{N}{2}}\exp(-\sigma\psi), \end{aligned}$$

where

$$(16)\quad \psi = \sum_{i=1}^r\sum_{j=1}^{n_i}\sum_{k=1}^{m_{ij}}\frac{(y_{ijk}-\eta_0\theta^{h_i}\lambda_{ijk})^2}{2\eta_0^2\theta^{2h_i}y_{ijk}} := \frac{\alpha_\theta}{\eta_0^2} - \frac{\beta_\theta}{\eta_0} + \gamma,$$

with

$$\alpha_\theta = \sum_{i=1}^r\sum_{j=1}^{n_i}\sum_{k=1}^{m_{ij}}\frac{y_{ijk}}{2\theta^{2h_i}},\ \beta_\theta = \sum_{i=1}^r\frac{\lambda_i}{\theta^{h_i}},\ \gamma = \sum_{i=1}^r\sum_{j=1}^{n_i}\sum_{k=1}^{m_{ij}}\frac{\lambda_{ijk}^2}{2y_{ijk}}.$$

It is easy to see that ψ, α_θ, β_θ, γ and $4\alpha_\theta\gamma - \beta_\theta^2$ are all positive with probability 1. For the sake of simplicity we will take α and β to replace α_θ and β_θ hereafter.

Taking the integration of $\pi_J(\eta_0, \theta, \sigma|\boldsymbol{y})$ in (15) with respect to σ, we have

$$\begin{aligned} \pi_J(\eta_0, \theta|\boldsymbol{y}) &\propto \sqrt{a(\theta)}\eta_0^{-2}\int_0^{+\infty}\sigma^{\frac{N}{2}}\exp(-\sigma\psi)\mathrm{d}\sigma \\ &\propto \frac{\sqrt{a(\theta)}}{\eta_0^2\psi^{\frac{N}{2}+1}}. \end{aligned}$$

Note that, as $\theta \to +\infty$,

$$(17)\quad \alpha = O(\theta^{-2h_1}),\quad 4\alpha\gamma - \beta^2 = O(\theta^{-2h_1}),$$

(18) $\beta\sqrt{\alpha} = O(\theta^{-2h_1})$,

(19) $\sqrt{\alpha\beta}\sqrt{2\sqrt{\alpha\gamma}-\beta} = O(\theta^{-\frac{3}{2}h_1})O(\theta^{-\frac{1}{2}h_1}) = O(\theta^{-2h_1})$

where $f(x) = O(g(x))$ means that $\lim_{x\to\infty}\frac{f(x)}{g(x)} = c$ with c being a constant. Moreover, we get

$$\frac{1}{\psi} = \frac{1}{\frac{\alpha}{\eta_0^2}-\frac{\beta}{\eta_0}+\gamma} \le \frac{4\alpha}{4\alpha\gamma-\beta^2} = O(1), \tag{20}$$

and

(21)
$$\begin{aligned}\int_0^{+\infty}\frac{1}{\eta_0^2\psi}\mathrm{d}\eta_0 &= \int_0^{+\infty}\frac{1}{\gamma\eta_0^2-\beta\eta_0+\alpha}\mathrm{d}\eta_0\\ &= \frac{2}{\sqrt{4\alpha\gamma-\beta^2}}\left(\frac{\pi}{2}+\arctan\frac{\beta}{\sqrt{4\alpha\gamma-\beta^2}}\right)\\ &\le \frac{2\pi}{\sqrt{4\alpha\gamma-\beta^2}}.\end{aligned}$$

Therefore, integrating $\pi_J(\eta_0,\theta|\boldsymbol{y})$ over η_0 and θ, and using (17), (20) and (21) we obtain that

$$\begin{aligned}&\int_1^{+\infty}\int_0^{+\infty}\pi_J(\eta_0,\theta|\boldsymbol{y})\mathrm{d}\eta_0\mathrm{d}\theta\\ &\quad\propto \int_1^{+\infty}\sqrt{a(\theta)}\int_0^{+\infty}\frac{1}{\eta_0^2\psi^{\frac{N}{2}+1}}\mathrm{d}\eta_0\mathrm{d}\theta\\ &\quad\le \int_1^{+\infty}\sqrt{a(\theta)}\left(\frac{4\alpha}{4\alpha\gamma-\beta^2}\right)^{\frac{N}{2}}\frac{2\pi}{\sqrt{4\alpha\gamma-\beta^2}}\mathrm{d}\theta\\ &\quad< \int_1^{+\infty}O(\theta^{-\frac{1}{2}(h_1+h_2+2)})O(\theta^{h_1})\mathrm{d}\theta\\ &\quad= \int_1^{+\infty}O(\theta^{\frac{1}{2}(h_1-h_2)-1})\mathrm{d}\theta < \infty,\end{aligned}$$

the last inequality holds since $\frac{1}{2}(h_1-h_2)-1 < -1$. Thus, the proof of Theorem 4.1 is completed. □

A.4 Proof of Theorem 4.2

Proof. Under the prior π_{R_1}, the joint posterior distribution $\pi_{R_1}(\eta_0,\theta,\sigma|\boldsymbol{y})$ is proportional to

$$\sqrt{b(\theta)}\eta_0^{-\frac{3}{2}}\sigma^{\frac{N}{2}-1}\exp(-\sigma\psi),$$

which follows that

$$\pi_{R_1}(\eta_0,\theta|\boldsymbol{y}) \propto \frac{\sqrt{b(\theta)}}{\eta_0^{\frac{3}{2}}\psi^{\frac{N}{2}}}.$$

Note that the function $\psi = \psi(\eta_0,\theta)$ defined in (16), given θ, has the maximum value γ on $[\frac{\alpha}{\beta},+\infty)$. Moreover,

$$\int_0^{+\infty}\frac{1}{\eta_0^{\frac{3}{2}}\psi^{\frac{N}{2}}}\mathrm{d}\eta_0 = \int_0^{\alpha/\beta}\frac{1}{\eta_0^{\frac{3}{2}}\psi^{\frac{N}{2}}}\mathrm{d}\eta_0 + \int_{\alpha/\beta}^{+\infty}\frac{1}{\eta_0^{\frac{3}{2}}\psi^{\frac{N}{2}}}\mathrm{d}\eta_0.$$

The integration above can be divided into the following two cases:

(1) When $N=1$, then the integration

$$\int_0^{\alpha/\beta}\frac{1}{\eta_0^{\frac{3}{2}}\psi^{\frac{N}{2}}}\mathrm{d}\eta_0 = \int_0^{\alpha/\beta}\frac{1}{\sqrt{\eta_0(\gamma\eta_0^2-\beta\eta_0+\alpha)}}\mathrm{d}\eta_0 \tag{22}$$

is divergent.

(2) When $N\ge 2$, we have

$$\begin{aligned}\int_0^{+\infty}\frac{1}{\eta_0^{\frac{3}{2}}\psi^{\frac{N}{2}}}\mathrm{d}\eta_0 &= \int_0^{+\infty}\frac{\eta_0^{\frac{1}{2}}}{\psi^{\frac{N}{2}-1}(\gamma\eta_0^2-\beta\eta_0+\alpha)}\mathrm{d}\eta_0\\ &\ge \int_{\alpha/\beta}^{+\infty}\frac{\eta_0^{\frac{1}{2}}}{\psi^{\frac{N}{2}-1}(\gamma\eta_0^2-\beta\eta_0+\alpha)}\mathrm{d}\eta_0\\ &\ge \left(\frac{1}{\gamma}\right)^{\frac{N}{2}-1}\int_{\alpha/\beta}^{+\infty}\frac{\eta_0^{\frac{1}{2}}}{\gamma\eta_0^2-\beta\eta_0+\alpha}\mathrm{d}\eta_0\\ &:= \left(\frac{1}{\gamma}\right)^{\frac{N}{2}-1}\tau(\theta).\end{aligned}$$

It can be shown that

$$\begin{aligned}&\tau(\theta)\\ &= \frac{1}{\sqrt{\gamma}\sqrt{2\sqrt{\alpha\gamma}-\beta}}\left[\frac{\pi}{2}-\arctan\left(\frac{\alpha\sqrt{\gamma}-\beta\sqrt{\alpha}}{\sqrt{\alpha\beta}\sqrt{2\sqrt{\alpha\gamma}-\beta}}\right)\right]\\ &+\frac{1}{\sqrt{\gamma}\sqrt{2\sqrt{\alpha\gamma}+\beta}}\log\left(\frac{\alpha\sqrt{\gamma}+\beta\sqrt{\alpha}+\sqrt{\alpha\beta}\sqrt{2\sqrt{\alpha\gamma}-\beta}}{\alpha\sqrt{\gamma}+\beta\sqrt{\alpha}-\sqrt{\alpha\beta}\sqrt{2\sqrt{\alpha\gamma}-\beta}}\right)\\ &\ge \frac{1}{\sqrt{\gamma}\sqrt{2\sqrt{\alpha\gamma}-\beta}}\left[\frac{\pi}{2}-\arctan\left(\frac{\alpha\sqrt{\gamma}-\beta\sqrt{\alpha}}{\sqrt{\alpha\beta}\sqrt{2\sqrt{\alpha\gamma}-\beta}}\right)\right].\end{aligned}$$

From (18) and (19), we have

$$\arctan\left(\frac{\alpha\sqrt{\gamma}-\beta\sqrt{\alpha}}{\sqrt{\alpha\beta}\sqrt{2\sqrt{\alpha\gamma}-\beta}}\right) = O(1),$$

it follows that

$$\tau(\theta) = O(\theta^{\frac{1}{2}h_1}).$$

Then the integration of $\pi_{R_1}(\theta|\boldsymbol{y})$ with respect to θ on interval $[1,+\infty)$ is not convergent, since

$$\sqrt{b(\theta)}O(\theta^{\frac{1}{2}h_1}) = O(\theta^{-1}), \quad (\theta\to+\infty).$$

Therefore, the posterior distributions $\pi_{R_1}(\eta_0,\theta,\sigma)$ under the reference prior π_{R_1} is improper. Similarly, we can obtain the same result for $\pi_{R_2}(\eta_0,\theta,\sigma)$. □

A.5 Proof of Theorem 4.3

Proof. It is readily shown that the marginal posterior distributions of the parameters (η_0, θ), under priors π_{R_3} and π_{R_M}, are given by

$$\pi_{R_3}(\eta_0, \theta|\boldsymbol{y}) \propto \eta_0^{-\frac{3}{2}} \psi^{-\frac{N}{2}} \sqrt{\frac{a(\theta)}{c(\theta)}},$$

$$\pi_M(\eta_0, \theta|\boldsymbol{y}) \propto \eta_0^{-\frac{3}{2}} \psi^{-\frac{N}{2}} \frac{\sqrt{a(\theta)b(\theta)}}{d(\theta)},$$

respectively. Following the case (1) in the proof of Theorem 4.2, we can obtain that the integration (22) diverges when $N = 1$, which means that the posteriors $\pi_{R_3}(\eta_0, \theta, \sigma|\boldsymbol{y})$ and $\pi_M(\eta_0, \theta, \sigma|\boldsymbol{y})$ are both improper.

When $N \geq 2$, however, we have

$$\begin{aligned} &\int_0^{+\infty} \frac{\eta_0^{\frac{1}{2}}}{\psi^{\frac{N}{2}-1}(\gamma\eta_0^2 - \beta\eta_0 + \alpha)} \mathrm{d}\eta_0 \\ &\leq \left(\frac{4\alpha}{4\alpha\gamma - \beta^2}\right)^{\frac{N}{2}-1} \int_0^{+\infty} \frac{\eta_0^{\frac{1}{2}}}{\gamma\eta_0^2 - \beta\eta_0 + \alpha} \mathrm{d}\eta_0. \end{aligned} \tag{23}$$

Using the formula 3.252.9 in [8], we obtain that

$$\begin{aligned} \int_0^{+\infty} \frac{\eta_0^{\frac{1}{2}}}{\gamma\eta_0^2 - \beta\eta_0 + \alpha} \mathrm{d}\eta_0 &= \frac{\pi}{\sqrt{\gamma}\sqrt{2\sqrt{\alpha\gamma} - \beta}} \\ &= O(\theta^{\frac{1}{2}h_1}). \end{aligned} \tag{24}$$

Furthermore, it can be shown that

$$\sqrt{\frac{a(\theta)}{c(\theta)}} = O(\theta^{-\frac{h_2+2}{2}}), \quad \frac{\sqrt{a(\theta)b(\theta)}}{d(\theta)} = O(\theta^{-\frac{h_2+2}{2}}). \tag{25}$$

From (23)–(25), we get

$$\begin{aligned} &\int_1^{+\infty}\int_0^{+\infty} \pi_{R_3}(\eta_0, \theta|\boldsymbol{y}) \mathrm{d}\eta_0 \mathrm{d}\theta \\ &\quad < \int_1^{+\infty} O(\theta^{-\frac{h_2+2}{2}}) O(\theta^{\frac{1}{2}h_1}) \mathrm{d}\theta \\ &\quad = \int_1^{+\infty} O(\theta^{\frac{1}{2}(h_1-h_2)-1}) \mathrm{d}\theta < \infty, \end{aligned}$$

and

$$\int_1^{+\infty}\int_0^{+\infty} \pi_M(\eta_0, \theta|\boldsymbol{y}) \mathrm{d}\eta_0 \mathrm{d}\theta < \infty.$$

which yields the desired result. □

ACKNOWLEDGEMENTS

The authors would like to thank the Editor, the Associate Editor and the two reviewers for their valuable comments which have greatly improved the quality of an earlier version of the paper.

Received 10 March 2018

REFERENCES

[1] Albert, J. (2009). *Bayesian Computation with R*. 2rd ed. Springer Science, New York. MR2839312

[2] Bagdonavičius, V. and Nikulin, M.S. (2000). Estimation in degradation models with explanatory variables. *Lifetime Data Analysis.* **7** 85–103. MR1819926

[3] Berger, J. O. (2006). The case for objective Bayesian analysis (with discussion). *Bayesian Analysis.* **1** 385–402. MR2221271

[4] Berger, J. O., Benardo, J. M. and Sun, D. C. (2009). The formal definition of reference priors. *Annals of Statistics.* **37**(2) 905–938. MR2502655

[5] Bernardo, J. M. (1979). Reference posterior distributions for Bayesian inference. *Journal of the Royal Statistical Society: Series B.* **41** 113–128. MR0547240

[6] Datta, G. S. and Ghosh, M. (1995). Some remarks on noninformative priors. *Journal of the American Statistical Association.* **90** 1357–1363. MR1379478

[7] Datta, G. S. (1996). On priors providing frequentist validity of Bayesian inference for multiple parametric functions. *Biometrika.* **83**(2) 287–298. MR1439784

[8] Gradshteyn, I. S. and Ryzhik, I. M. (2007). *Table of Integrals,Series and Products*, 7th ed. Academic Press. MR0669666

[9] Guan, Q., Tang, Y. C. and Xu, A. C. (2015). Objective Bayesian analysis accelerated degradation test based on Wiener process models. *Applied Mathematical Modelling.* **40**(4) 2743–2755. MR3454490

[10] He, L., He, D. J. and Cao, M. X. (2016). Objective Bayesian analysis of degradation model with respect to a Wiener process. *Journal of Systems Science and Complexity.* **29** 1737–1751. MR3582049

[11] Hu, C. H., Lee, M. Y. and Tang, J. (2015). Optimum step-stress accelerated degradation test for Wiener degradation process under constraints. *European Journal of Operational Research.* **241**(2) 412–421. MR3276771

[12] Jeffreys, H. (1961). *Theory of Probability*, 3rd ed. Oxford: Oxford University Press. MR0187257

[13] Lawless, J. and Crowder, M. (2004). Covariates and random effects in a gamma process model with application to degradation and failure. *Lifetime Data Analysis.* **10** 213–227. MR2086957

[14] Ling, M. H., Tsui, K. L. and Balakrishnan, N. (2015). Accelerated degradation analysis for the quality of a system based on the gamma process. *IEEE Transactions on Reliability.* **64**(1) 463–472.

[15] Meeker, W. Q. and Escobar, L. A. (1998). *Statistical Methods for Reliability Data*. Wiley, NewYork.

[16] Nelson, W. (1990). *Accelerated Testing: Statistical Models, Test Plans, and Data Analyses*. Wiley, New York.

[17] Neal, P. and Roberts, G. (2008). Optimal scaling for random walk metropolis on spherically constrained target densities. *Methodology & Computing in Applied Probability.* **10** 277–297. MR2399684

[18] Pan, Z. and Balakrishnan, N. (2011). Reliability modeling of degradation of products with multiple performance characteristics based on gamma process. *Reliability Engineering & System Safety.* **96** 949–957.

[19] Peng, C. Y. (2015). Inverse Gaussian processes with random effects and explanatory variables for degradation data. *Technometrics.* **57**(1) 100–111. MR3318353

[20] Tsai, C. C., Tseng, S. T. and Balakrishnan, N. (2012). Optimal design for gamma degradation processes with random effects. *IEEE Transactions on Reliability.* **61** 604–613.

[21] Tseng, S. T., Balakrishnan, N. and Tsai, C. C. (2009). Optimal step-stress accelerated degradation test plan for gamma degradation processes. *IEEE Transactions on Reliability.* **58** 611–618.

[22] Wang, H., Wang, G. J. and Duan, F. J. (2016). Planning of step-stress accelerated degradation test based on the inverse Gaussian process. *Reliability Engineering & System Safety.* **154**

97–105.

[23] Wang, X. and Xu, D. (2010). An inverse Gaussian process model for degradation data. *Technometrics*. **52** 188–197. MR2676425

[24] Wang, X., Balakrishnan, N. and Guo, B. (2014). Residual life estimation based on a generalized Wiener degradation process. *Reliability Engineering & System Safety*. **124** 13–23.

[25] Wasan, M. (1968). On an inverse Gaussian process. *Scandinavian Actuarial Journal*. **68**(2) 69–96.

[26] Whitmore, G. A. (1995). Estimating degradation by a Wiener diffusion process subject to measurement error. *Lifetime Data Analysis*. **1** 307–319.

[27] Whitmore, G. A. and Schenkelberg, F. (1997). Modeling accelerated degradation data using Wiener diffusion with a time scale transformation. *Lifetime Data Analysis* **3** 27–45.

[28] Xu, A. C. and Tang, Y. C. (2012). Objective Bayesian analysis for linear degradation models. *Communications in Statistics-Theory and Methods*. **41** 4034–4046. MR2973640

[29] Ye, Z. S. and Chen, N. (2014). The inverse Gaussian process as a degradation model. *Technometrics*. **56**(3) 302–311. MR3238068

[30] Ye, Z. S., Chen, L. P., Tang, L. C. and Xie, M. (2014). Accelerated degradation test planning using the inverse Gaussian process. *IEEE Transactions on Reliability*. **63**(3) 750–763.

[31] Ye, Z. S., Chen, N. and Shen, Y. (2015). A new class of Wiener process models for degradation analysis. *Reliability Engineering & System Safety*. **139** 58–67.

Lei He
Department of Statistics
Anhui Normal University
Wuhu 241003 China
E-mail address: lhstat@163.com

Dongchu Sun
Department of Statistics
University of Missouri-Columbia
Missouri 65211 US
Department of Statistics
East China Normal University
Shanghai 200241 China
E-mail address: sund@missouri.edu

Daojiang He
Department of Statistics
Anhui Normal University
Wuhu 241003 China
E-mail address: djheahnu@163.com